University of North Carolina Asheville
Journal of Undergraduate Research
Asheville, North Carolina
May 2019

Importance of Isoleucine 55 for Rotor-Stator Interactions in *E. coli* F_1F_O ATP Synthase

Michaela Dodd
Chemistry
University of North Carolina Asheville
One University Heights
Asheville, North Carolina 28804 USA

Faculty Advisor: Dr. P. Ryan Steed

Abstract

ATP synthase (ATPase), a ubiquitous biological nanomachine, is responsible for synthesizing the majority of adenosine triphosphate (ATP) in cells. The process of synthesizing ATP uses a unique rotary mechanism, which involves two motors, F_1 and F_O where protons translocated through F_O generate torque to drive F_1 to synthesize ATP from ADP and P_i. Previous studies in *Escherichia coli* (*E. coli*) ATP synthase showed that proton translocation occurs at the subunit *a/c* interface (located in F_O) and that some amino acid residues in this region are important for function. We are attempting to elucidate what chemical properties are essential for functionality of the isoleucine at position 55 (cI55), which is located on the second transmembrane helix (TMH2) of subunit *c*. Changes in the side chain were imposed using site directed mutagenesis via polymerase chain reactions (PCR) or through chemical modifications with methanethiosulfonate reagents. ATP-driven H^+ pumping activity was observed using fluorescence spectroscopy. So far, replacing isoleucine with glycine, alanine, valine, leucine, and phenylalanine (*c*I55G, *c*I55A, *c*I55V, *c*I55L, and *c*I55F) resulted in H^+ pumping that behaves similarly to that of the wild type. Proton permeability was also assayed on mutations *c*I55G, *c*I55A, *c*I55F which closely resemble the activity of wild type. Additionally, chemical modifications that increased the steric bulk of the cysteine mutant by adding methyl, propyl, butyl, and benzyl side chains were unable to restore function. These results suggest that if a hydrophobic residue is at this position, ATP synthase can function, regardless of the bulkiness of the amino acid side chain. Mutations to determine if there is an interdependence of *c*I55 with the adjacent phenylalanine 54 (*c*F54) as well as the effect that sulfur has at this position are in progress.

1. Introduction

Adenosine triphosphate (ATP) is the universal chemical energy currency for all life (Figure 1).[1,2] ATP synthase (ATPase), a biological nanomachine, is responsible for creating the majority of ATP in cells using a unique rotary mechanism that takes advantage of the proton gradient across the cell membrane.[3] This mechanism generates rotation that induces conformational changes that catalyze the synthesis of ATP.[4] The biological nanomachine is composed of three main functional components that work in tandem: the rotor, the stator, and the headpiece. [2]

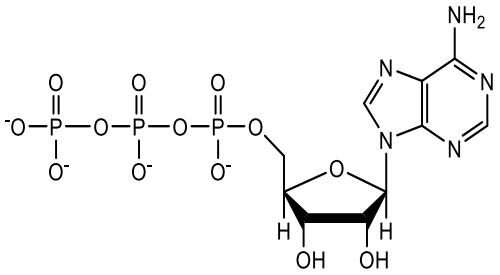

Figure 1. Chemical structure of adenosine triphosphate (ATP).

In *Escherichia coli* (*E. coli)*, the rotor is composed of γ, δ, and ε subunits as well as the membrane-embedded *c*-ring, all of which work together to rotate as protons enter and exit. The stator is composed of the *a* subunit and the b_2 stabilizing arm which allows protons to enter and exit F_O via two half-channels as shown in Figure 2. ATP synthesis occurs in the headpiece through conformational changes within the hexameric $\alpha_3\beta_3$ subunit.[1,3,5,6] These three main functional units can be categorized into the two major components: F_1 and F_O of the ATPase.

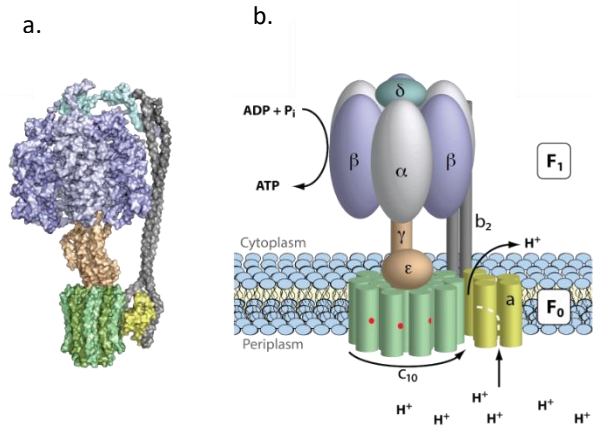

Figure 2: a. The structure of F_1F_O ATPase (5T4O) b. A cartoon structure of F_1F_O ATPase with all subunits labeled.[7]

1.1 F_1 Sector

F_1 is located inside the cell, contains a multi-subunit structure with a $\alpha_3\beta_3\gamma\delta\varepsilon$ ratio, and possesses three active sites for ATP synthesis and hydrolysis.[1–3] In the binding change mechanism, conformational changes occur at the three active sites which are located at the α/β interfaces. Each active site proceeds through three states: loose, tight, and open as depicted in Figure 3.[1] The loose state binds adenosine diphosphate (ADP) and inorganic phosphate (P_i). The tight state isoenergetically creates an environment in which ADP and P_i are converted to ATP and H_2O. In the open state, ATP is expelled into the cell.

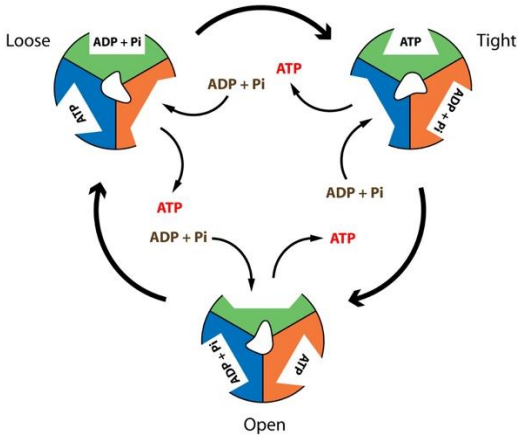

Figure 3. Induced conformational changes that the active sites undergo (loose, tight, and open).[8]

1.2 F_O Sector

F_O is embedded in the membrane and is composed of subunits *a*, *b*, and *c*. Subunit *a* is composed of five α-helices, and helices 2-5 form a four-helix bundle that forms the *a/c* interface with subunit *c*. The *E. coli c* ring is decameric and each *c* subunit folds in a hairpin like structure with two α-helices connected by a polar loop (Figure 4a). The α-helices are oriented so that transmembrane helix 1 (TMH1) is located on the inside of the ring while TMH2 is located on the surface. Subunit *a* serves as the entry half channel while the exit half channel is located at the *a*/*c* interface (Figure 4b).[1,2,4–6,9]

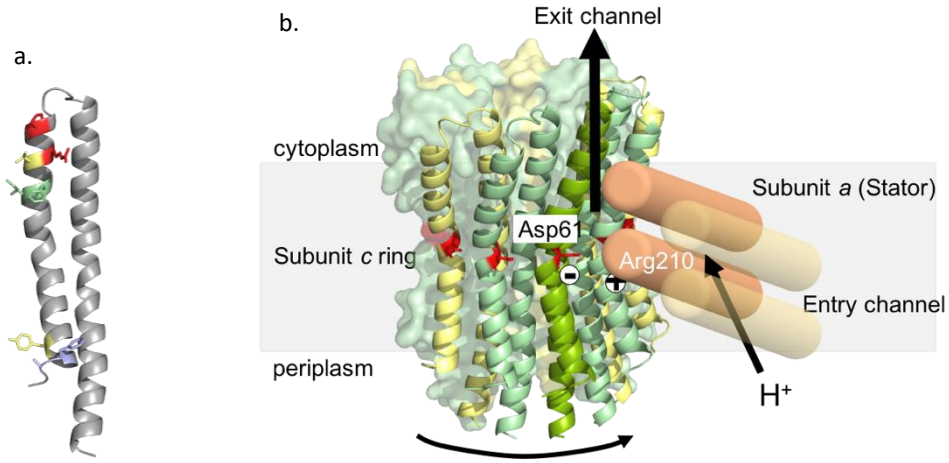

Figure 4. a. Shape of one *E. coli c* subunit. b. A zoomed in view of the *a/c* interface.

This figure illustrates that protons enter the stator, subunit a of F_O using an entry half-channel. When the proton encounters the conserved arginine residue which is positively charged in subunit *a*, it translocates to subunit *c*, the rotor. Due to the discontinuous channel, protons are forced to rotate about the c-ring before they can exit using the exit half-channel located at the *a/c* interface. They then travel through the gamma stalk up to F_1 where ATP is synthesized or hydrolyzed.

1.3 Background

While much is known about the F_1 mechanism, what drives the rotation of F_O is unclear. Prior research on the mechanism that drives rotation involved systematically changing various amino acids to determine their importance

and determination of the structure of the Fo motor.[3,10] This process allows researchers to gain a better understanding as to what properties are crucial to this protein complex's function such as hydrophobicity, sterics, etc. as well as insight to its structure. Lightowlers et al. performed mutagenic substitutions by substituting *a*Arg210 →Gln, *a*His 245 → Leu, and Lys 167 and Lys 169 → Gln and their results led them to determine that helices 4 and 5 of subunit *a* and helix 2 of subunit *c* interactions are integral to a functional ATPase.[11] Jiang and Fillingame performed cross-linking experiments allowing them to see how different parts of the protein complex interact with each other. Their results yielded the positions of the *a* and *c* subunits, specifically that helix 2 of subunit *c* faces helix 4 of subunit *a*.[12] Advances in structural imaging techniques, such as cryo-electron microscopy (Cryo-EM) provided the first medium resolution structural data of *E. coli* ATP synthase giving insight into what aspects of ATP synthase need to be further studied.

One hypothesis for torque generation is a ratchetting mechanism, Figure 5, in which helices 4-5 of subunit *a* would undergo a conformation change due to the pH of the periplasm, breaking the salt bridge that is between *a*Arg210 on *a*TMH4 and *c*Asp61 on *c*TMH2 allowing a proton entry into the periplasmic half channel. After the proton enters, *a*TMH4 and *a*TMH5 swivel granting the proton access to cAsp61. As the *a* subunit reverts back to its original conformation the proton gets ejected out via a different half channel into the cytoplasm, and the c-ring moves forward one step.[4]

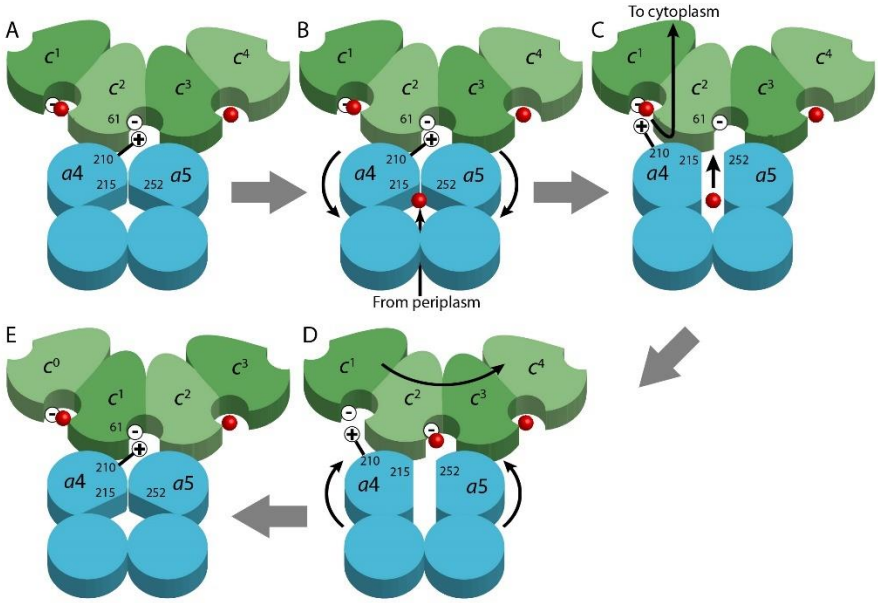

Figure 5. Shows the mechanism for which protons get translocated using a ratchetting mechanism.

Genetically modifying residues that seem to be critical for function is another way to determine how *a/c* interface interactions affect ATPase. Fillingame and colleagues focused on mapping the proton exit channel by performing a cysteine scan in which they strategically substituted each amino acid residue on the *c* subunit with a cysteine residue and measured aqueous accessibility. Their results suggest that the amino acids located at the 47, 50, 51, 54, 55, 73, 76, and 77 positions are involved in the mechanism that drives ATP and require more in-depth research.[5,6,9] Weidenmann et al. measured the fluorescence of pyranine over time and determined that the rates of proton flux through F_O are different in the ATP synthesis and hydrolysis directions.[13] These results then lead to the idea that there are two different mechanisms in operation: one for ATP synthesis and another mechanism for ATP hydrolysis.[5,6,12,13] Unpublished results from the Steed lab tested for H^+ permeability and ATPase activity; their results showed that all Cys substitutions except for F75 and A77 yielded channel blockage and arrested rotation, whereas F76C resulted in rotor disengagement, and A77C remained functional.

In the Steed Research Group, former students tested chemical determinants of rotor-stator interactions in *E. coli* F_1F_O ATP synthase. Their starting material was an already mutated phenylalanine to cysteine which showed a loss in proton pumping functionality. By imposing chemical modifications using MTS reagents to add a methyl, propyl, and benzyl substituents, they were able to restore some functionality. Successful restoration of proton functionality determined that steric bulk at this position (*c*54) is chemically necessary for ATP synthase. These results can be used

as a springboard to further research of *c*I55, which is located on the same α-helix as *c*F54 and would be expected to behave in a similar manner.

The main goal of this research is to determine how cI55 contributes to the torque that is generated on the rotor via proton translocation through the *E. coli* F_O motor. This research specifically looks at how altering *c*I55 and its position on the *c*-ring surface impact ATP synthase function. These mutants will be tested using biological assays that will test for ATP synthesis and ATP hydrolysis. The purpose behind testing the mutant in both types of assays is to determine whether there are two mechanisms at play, one for the forward direction, ATP synthesis, and a different one for the reverse direction, ATP hydrolysis. The results of this research could then be extrapolated towards the advancement of medical research regarding how antibiotics, like Bedaquiline, inhibit ATP synthesis in mycobacteria by binding at the *a/c* interface.[14]

2. Experimental Methods

2.1 Generation of mutants

Mutants were constructed in plasmid pCMA113, in which all native cysteines in the nine encoding F_1F_O subunits are replaced with either alanine or serine. Site directed mutagenesis of *c*I55 to various amino acids was performed using 2-step megaprimer PCR method,[15] utilizing oligonucleotides with a single point mutation allowing for changes in the codon and thus the encoded amino acid residue. The lengths of the PCR fragments were confirmed using agarose gel electrophoresis. The product was purified using a Monarch PCR clean up kit (NEB) and digested using restriction enzymes PpuM1 and BsrG1. The digested products were then purified by gel electrophoresis, ligated into a plasmid, and transformed into JWP292, an *E. coli* strain in which genes encoding ATP synthase have been deleted from the genome, Figure 6.

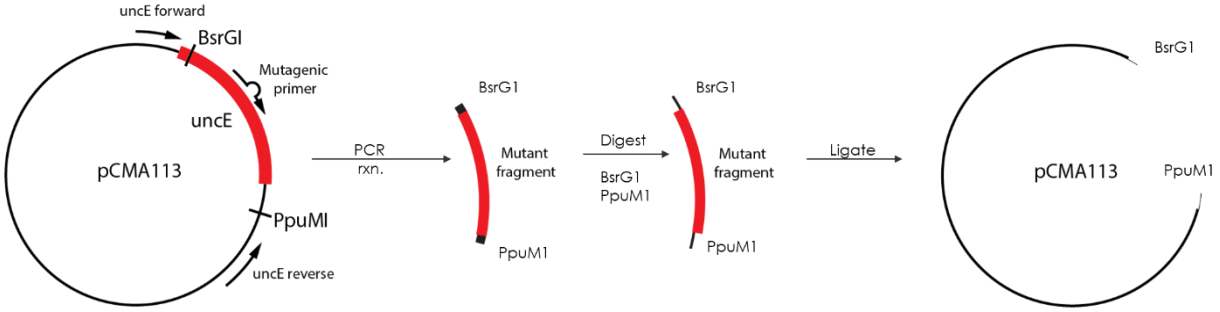

Figure 6: A visual workflow on mutagenesis.

2.2 Preparation of Inside-out (ISO) and Stripped Vesicles

Large cultures of transformed JWP292 *E. coli* were prepared in M63-TAUD minimal medium (618 mM KH_2PO_4(mono), 382 mM K_2HPO_4 (dibasic), 10 mM $MgSO_4$, 150 mM $(NH_4)_2SO_4$, 5 mg/L $FeSO_4$, and TAUD (0.005 mg/mL thiamine, 0.2 mM arginine, 0.2 mM uracil, 0.02 mM dihydroxybenzoate). Cells were harvested by centrifugation at 4000 rpm for 15 minutes and resuspended via vortex mixing using TMG buffer (50 mM Tris, 5.0 mM $MgCl_2$, 10% v/v glycerol, pH 7.5) with 1 mM dithiothreitol (DTT). Cells were then lysed using a high-pressure homogenizer at 18,000 psi ($\geq$3 passes). Lysed cells were centrifuged at 9000 x g for 10 minutes to remove cell debris, and the supernatant was subsequently centrifuged at 193,000 x g for 60 minutes to collect the membrane vesicles. The pellet was resuspended in TMG buffer via a glass dounce, aliquoted into microcentrifuge tubes, and stored at -80°C.[5] Stripped vesicles were prepared using ISO vesicles. F_1 was chemically stripped off by using TEDG (1mM Tris-OAc, pH 9, 0.5 mM Na_2EDTA, 1mM DTT, 10% glycerol) buffer and collected with multiple rounds of centrifugation.

2.3 Protein Concentration Determination

To determine protein concentration, ISO vesicles were diluted (25x) with water, and a bovine serum albumin (BSA) standard was prepared using dilutions of 0.65 mg/mL BSA. Standards and membrane samples in triplicate were treated with $CuSO_4$ in basic solution and oxidized with Folin-Ciocalteu, color developed at room temperature for 30-45 minutes, and absorbance was read at 650 nm. [16]

2.4 ATP driven H^+ Pumping Assay

Aliquots of ISO vesicles were diluted to 10 mg/mL with TMG buffer. Membrane vesicles, 0.3 µg/mL 9-amino-6-chloro-2-methoxyacridine (ACMA), and 3.2 mL HMK buffer (50 mM HEPES, 5.0 mM $MgCl_2$, 300 mM KCl, pH 7.5) were combined, vortexed and then transferred to cuvettes to observe fluorescence (λ_{ex}= 415 nm, λ_{em}= 485 nm) in an AMINCO·Bowman Series 2 Luminescence Spectrometer. Proton pumping into the lumen of the ISO vesicles was initiated by the addition of 30 µL of 25 mM ATP at 20 seconds and terminated at 100 seconds with 0.5 µg/mL nigericin, an uncoupler.[6]

2.5 Thiolate Modification and DTNB Assay

Methyl, propyl, butyl, and benzyl-methanethiosulfonate (1mM) in DMSO, Figure 7a, and N-ethylmaleimide (1 mM) in EtOH, Figure 7b, reagents were added to the cysteine-substituted F_1F_O vesicles, incubated at room temperature for 15 minutes, and tested for H^+ pumping.

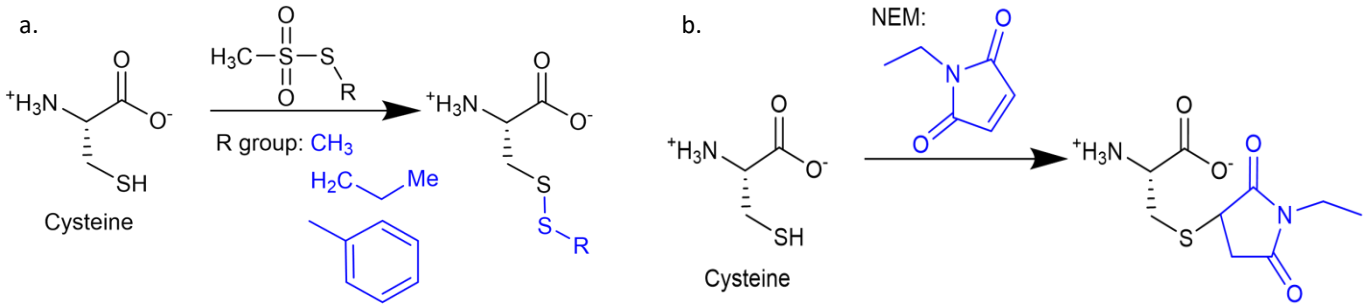

Figure 7a.Chemical reaction scheme for MTS modifications. b. Chemical reaction scheme for a Michael Addition of NEM.

Afterwards, membrane aliquots were diluted to 1 mg/mL with TMG buffer. To measure the extent of the MTS modification, 0.5 mg/mL of vesicles, 1% SDS, 0.2 mM (DTNB) dithio-bis (2-nitrobenzoic acid), and TMG were added, mixed and incubated for 15 minutes before absorbance was read at 412 nm (Figure 8).[17]

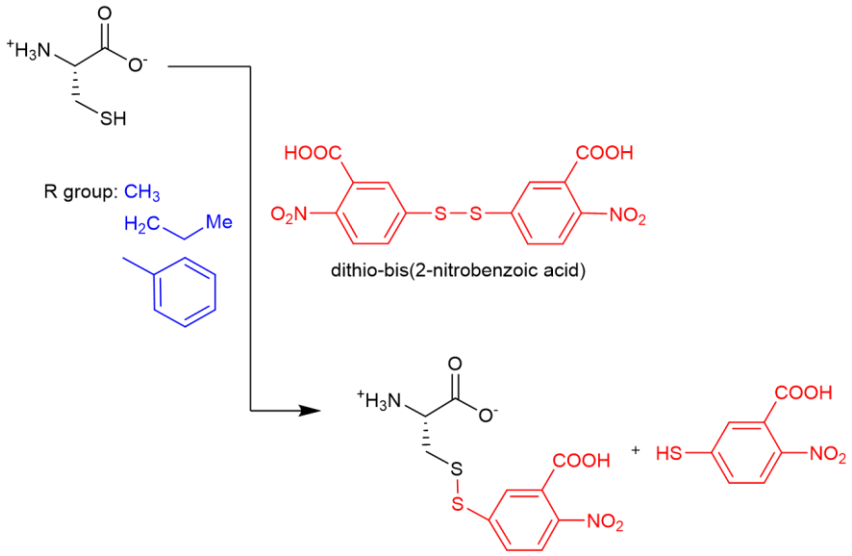

Figure 8: The reaction scheme for unreacted cysteines using DTNB.

2.6 H^+ Permeability of Stripped ISO Membrane Vesicles

Stripped membrane vesicles, quinacrine 6.0 mg/mL, and 3.2 mL HMK buffer were combined, vortexed and then transferred to cuvettes to observe fluorescence ($\lambda_{ex=}$ 415 nm, λ_{em}= 496 nm) in the AMINCO·Bowman Series 2 Luminescence Spectrometer. Proton pumping into the lumen of the ISO vesicles was initiated by the addition of 16 µL of 10mM NADH at 20 seconds and terminated at 100 seconds with 5 µg/mL nigericin, an uncoupler.[6]

2.7 Succinate Growth Assay

Small 5 mL M63-TAUD culture tubes were prepared. Next the tubes were inoculated with frozen glycerol stock and incubated overnight at 37°C with shaking at 240 rpm. The following morning the cultures were serially diluted 1:10,000 with 1x M63 buffer and 100 µL was plated and evenly spread onto a rich medium LB agar plate and a succinate agar plate (M63-TAUD, 20mM succinate) and incubated for 16 and 72 hours respectively. After the appropriate amount of time, the colony size on the succinate plates was observed and recorded in mm.

3. Results and Discussion

3.1 Generating New Mutants

We used PCR mutagenesis to construct four mutations at position Ile55: glycine (*c*I55G), valine (*c*I55V), phenylalanine (*c*I55F), and tryptophan (*c*I55W). PCR fragments were subjected to purification, digestion, ligation, and transformation into DH5α submitted for sequencing to confirm mutants produced (Figure 9).

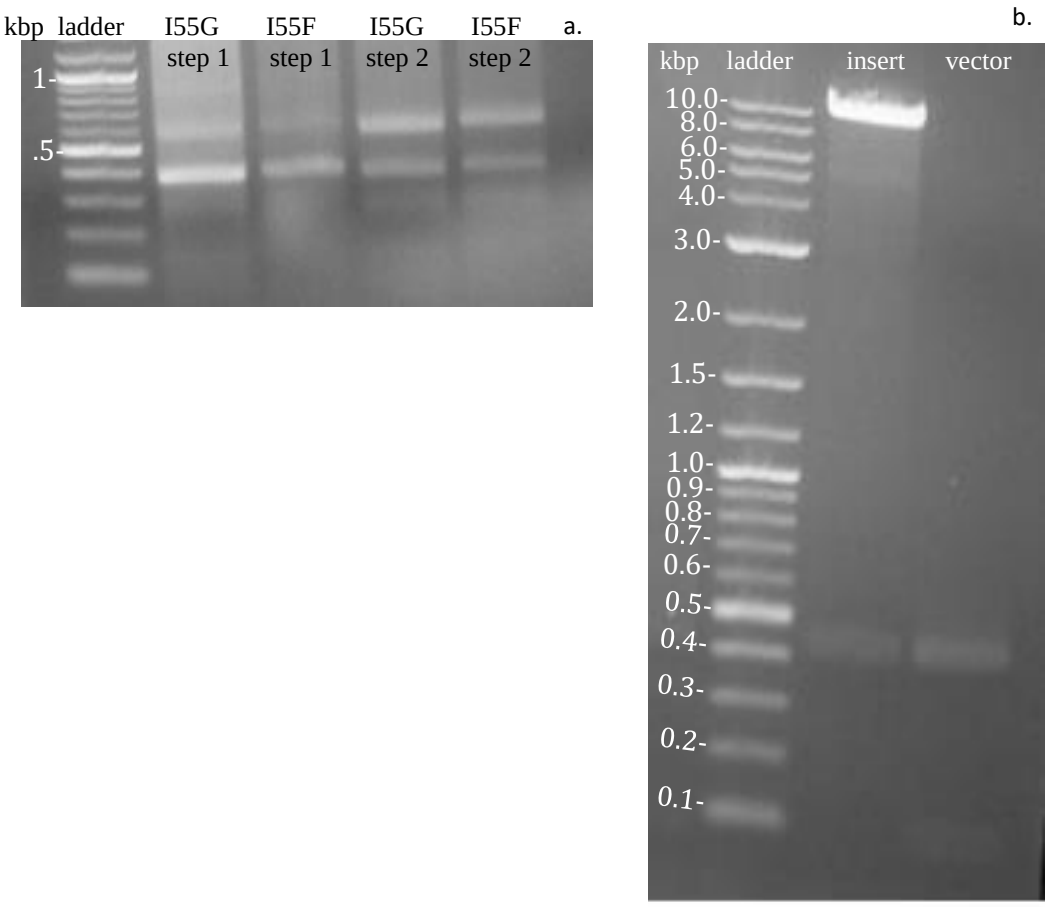

Figure 9. a. An example of a diagnostic gel: 2 µL samples (+3 µL water, 1 µL loading dye) 1% agarose, 0.5µg/mL ethidium, 1x TAE, 110 V. In lanes 1, 2-5 are the ladder and mutant fragments respectively.

Step 1 product is about 400 bp in length while step 2 is about 600 bp in length. b. An example of a digestion gel: 30 µL samples (+ 10 µL loading dye) 1% agarose, 0.5µg/mL ethidium, 1x TAE, 90 V. In lanes 1-3 are the ladder, the vector, and the mutant respectively. The vector is about 10.0 kilobase pairs (kbp) and the insert is about 0.4-0.5 kbp in length.

3.2 Function of Mutants in ATP-Driven H^+ Pumping

We determined the ATP-driven H^+ pumping activity of the genetic mutants and results are shown below (Figure 10). The results of this assay show that regardless of which side chain is substituted for isoleucine, ATP synthase is still able to function with the cysteine being the exception. When cysteine is substituted for isoleucine, proton pumping is inhibited. Additionally, we did not expect the observed H^+ pumping behavior that alanine displayed at position 55 due to the lack of a bulky substituent coming off the amino acid backbone.

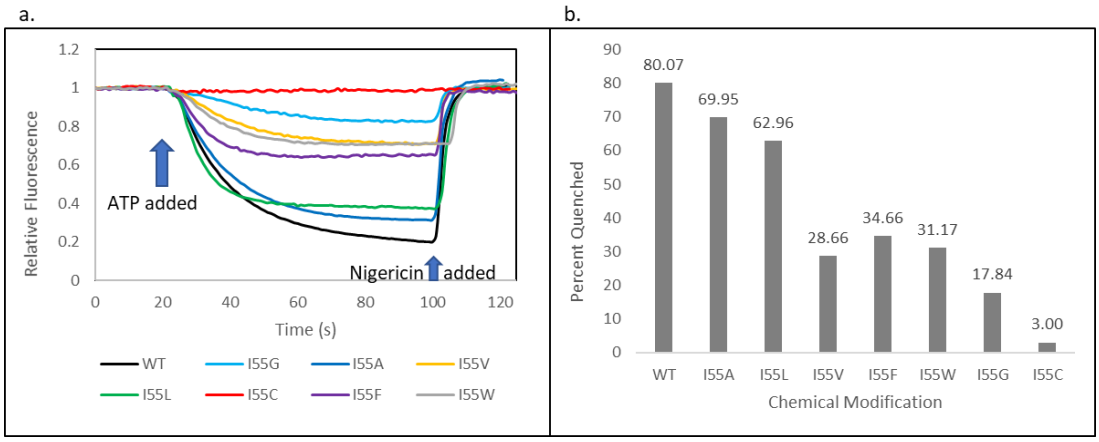

Figure 10. a. The effects of each genetically modified mutant on ATP-driven H^+ pumping compared to the wild type (cI55). WT: black, I55G: light blue, I55A: blue, I55V: yellow, I55L: green, I55C: red, I55F: purple, I55W: grey b. The H^+ pumping activity for each mutant compared to the wild type shown by the percentage of fluorescence quenched.

3.3 The Effects of Thiolate Modifications on ATP-driven H^+ Pumping

Attempts to restore function using thiolate reagents were unsuccessful as seen by the results of Figure 11. The graph below (Figure 11) shows the effects of thiolate modifications that were carried out using methyl MTS, propyl MTS, benzyl MTS and N-ethylmaleimide reagents on H^+ pumping. The results of the additions of the sterically bulky groups were not effective in restoring function. We did not expect the lack of restorative function observed H^+ pumping assay considering previous research on F54 was successful in restoring function when performing these chemical modifications.

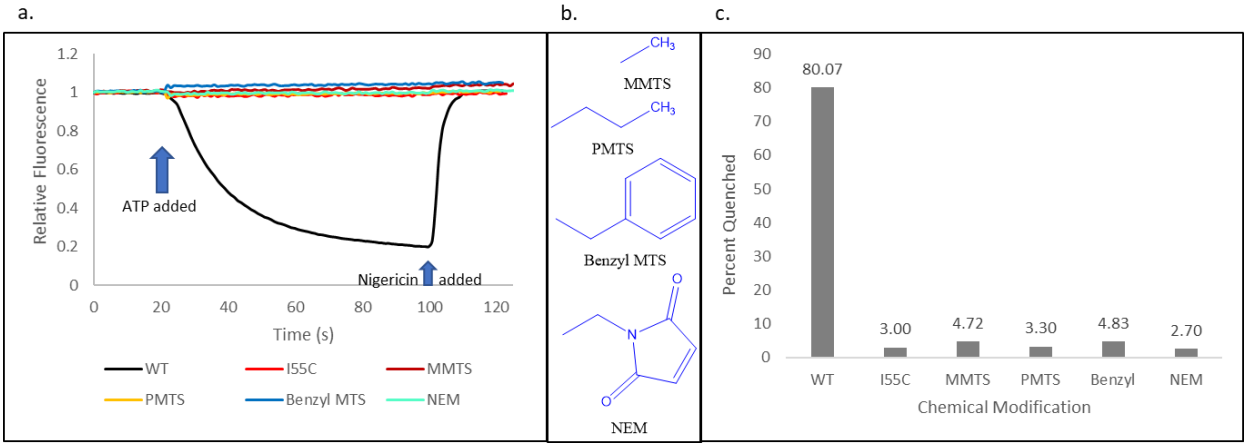

Figure 11 a. H^+ pumping fluorescence time trace shows the inability to restore functionality by the addition of sterically bulky groups to the cysteine substituted residue at position 55 of subunit c. WT: black, I55C: red, I55C_MMTS: brown, I55C_PMTS: yellow, I55C_BenzylMTS: blue, I55C_NEM: teal. b. Shows the various substituents that were added via the chemical modification. c. H^+ pumping quenching activity shows the fluorescence quenching activity for each mutant compared to the wild type and the cysteine mutant.

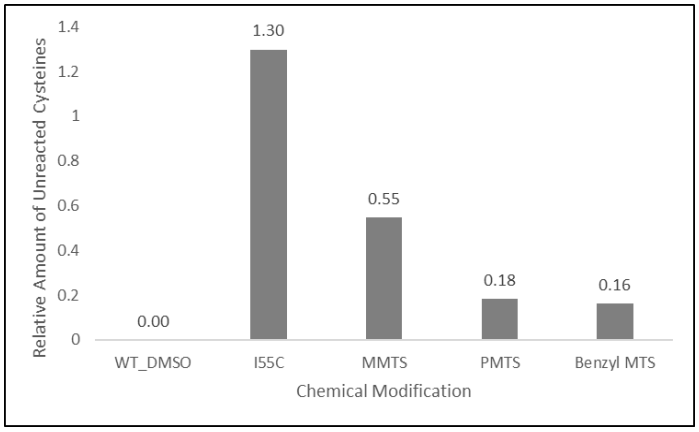

Figure 12. DNTB assay for unreacted cysteines shows that the MTS reagent did not react efficiently.

3.4 Effect of Mutants on H^+ Permeability

In order to determine whether mutations affect the passive translocation of H^+ through F_O, ISO vesicles are stripped, removing F_1 from the F_1F_O complex. The electron transport chain in the vesicle oxidizes NADH to generate the proton gradient, which will not form if F_O is permeable. The permeability of F_O can be described as one of the following three possible states: open, blocked, or partially blocked. Proton permeability is reported in Figure 13. In figure 13a., wild type and *c*I55G and *c*I55F show relatively the same activity with unchanged fluorescence reading for the entirety of the time trace. This result indicates that the c ring is free to rotate and as protons enter the c ring, freely translocating through access channels. For mutants, *c*I55A, *c*I55V, and *c*I55L, there is a slight increase in fluorescence response which is indicative of a partial blockage which still allows protons passage just not as easily as if the *c* ring were open. Lastly, for *c*I55C, there is a great increase in fluorescence response lending to the c-ring's inability to rotate, restricting the movement of protons across the membrane.

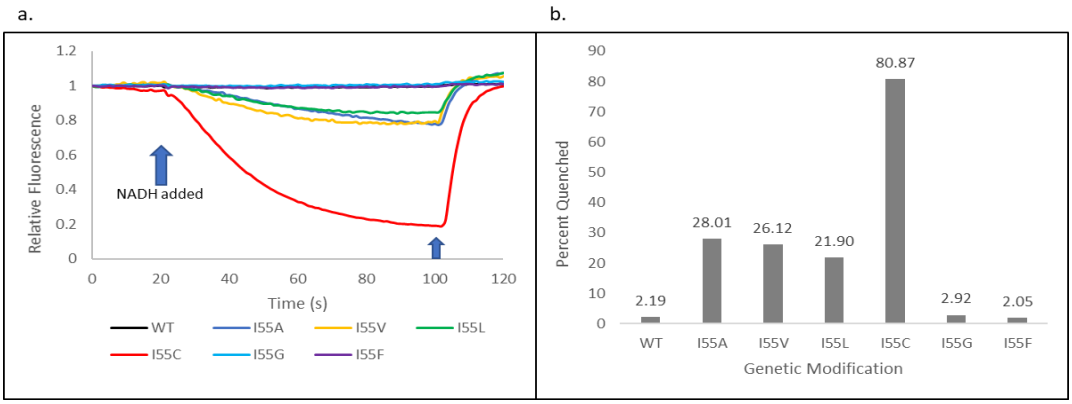

Figure 13. a. H^+ permeability time trace shows the effects of each mutant on H^+ permeability of F_1 via fluorescence quenching. WT: black, I55G: light blue, I55A: blue, I55V: yellow, I55L: green, I55C: red, I55F: purple, I55W: grey b. The H^+ permeability quenching activity for each mutant compared to the wild type.

3.5 Effect of Mutants on Succinate Growth in vivo

All mutants grew on succinate plates (Figure 14) showing that each mutant has a functional ATP synthase, including cysteine which is consistent with data from previous research. This result is puzzling, because although the cysteine

mutant grows on the succinate plates it does not perform well in the ATP-driven H^+ pumping assay and appears to block passive transport.

Mutant	Colony Size (mm)
WT	1-2 mm
I55G	1-2 mm
I55A	1-2 mm
I55V	1-2 mm
I55L	1-2 mm
I55C	1-2 mm
I55F	1-2 mm
I55W	1-2 mm

Table 1. Shows the measured diameters of colonies grown on succinate plates of different mutants compared to the wild type.

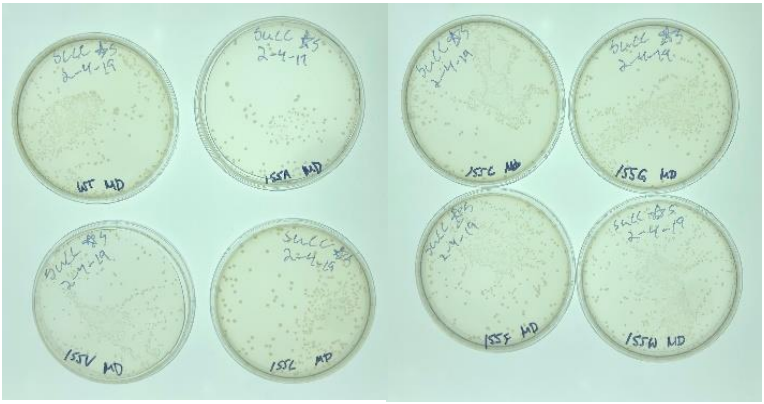

Figure 14. Shows the colony growth on succinate plates for the various mutants compared to the wild type.

4. Conclusion

According to the data, all mutants of *c*Ile55 result in a functional ATP synthase as observed by colony growth on succinate plates. I55 seems to tolerate any hydrophobic residue resulting in a functional ATP synthase in the hydrolysis direction with the except of cysteine. Cysteine uniquely inhibits proton pumping. Additionally, chemically modifying the cysteine substituted mutant with the cys-thiol reagents, ATP hydrolysis was unable to be restored, as seen in the lack of fluorescence quenching in the ATP-driven H^+ pumping assay. H^+ permeability of I55G and I55F show the same activity as wild type, I55A, I55V, I55L showed a partial blockage while the cysteine mutation showed that the c-ring is blocked which resulted in the increased response of fluorescence quenching measured. Overall, position cI55 seems to tolerate all hydrophobic substitutions except for cysteine. Cysteine seems to uniquely block function at this position and further research should be conducted to explain this result.

5. Future Research

Future experiments should include generating a methionine (*c*I55M), serine (*c*I55S), and a double alanine mutant with F54 (*c*F54A/*c*I55A), the adjacent amino acid residue. The serine mutant will just verify the importance of hydrophobicity at this position, the methionine mutant will test if the presence of a sulfur group is causing the blockage in the c ring rotation, and lastly, the double mutant will probe for the interdependence of *c*I55 on its adjacent amino acid residue *c*F54. Additionally, all *c*I55 mutants should be tested in the ATP synthesis direction using a Luciferin-Luciferase assay. Performing this assay would provide a complete data set in which the essential properties at position 55 could be determined while also elucidating the mechanism that drives F_O rotation.

6. Acknowledgements

I would like to thank Dr. Steed for his mentorship and guidance throughout this project, the University of North Carolina Asheville Undergraduate Research Program for funding this research, and the Steed Squad for their support and comradery.

7. References

(1) Sobti, M.; Smits, C.; Wong, A. S. W.; Ishmukhametov, R.; Stock, D.; Sandin, S.; Stewart, A. G. Cryo-EM Structures of the Autoinhibited E. Coli ATP Synthase in Three Rotational States. *Elife* **2016**, *5* (DECEMBER2016), 1–18. https://doi.org/10.7554/eLife.21598.

(2) von Ballmoos, C.; Wiedenmann, A.; Dimroth, P. Essentials for ATP Synthesis by $F_1 F_0$ ATP Synthases. *Annu. Rev. Biochem.* **2009**, *78* (1), 649–672. https://doi.org/10.1146/annurev.biochem.78.081307.104803.

(3) Yanagisawa, S.; Frasch, W. D. Protonation-Dependent Stepped Rotation of the F-Type ATP Synthase c-Ring Observed by Single-Molecule Measurements. *J. Biol. Chem.* **2017**, *292* (41), 17093–17100. https://doi.org/10.1074/jbc.M117.799940.

(4) Fillingame, R. H.; Steed, P. R. Half Channels Mediating H+ Transport and the Mechanism of Gating in the Fo Sector of Escherichia Coli F1Fo ATP Synthase. *Biochim. Biophys. Acta - Bioenerg.* **2014**, *1837* (7), 1063–1068. https://doi.org/10.1016/j.bbabio.2014.03.005.

(5) Steed, P. R.; Fillingame, R. H. Aqueous Accessibility to the Transmembrane Regions of Subunit c of the Escherichia Coli F1F0 ATP Synthase. *J. Biol. Chem.* **2009**, *284* (35), 23243–23250. https://doi.org/10.1074/jbc.M109.002501.

(6) Steed, P. R.; Fillingame, R. H. Residues in the Polar Loop of Subunit c in Escherichia Coli ATP Synthase Function in Gating Proton Transport to the Cytoplasm. *J. Biol. Chem.* **2014**, *289* (4), 2127–2138. https://doi.org/10.1074/jbc.M113.527879.

(7) P. R. Steed. F1FO ATP Synthase Cartoon, University of North Carolina Asheville, 2018.

(8) Steed, P. R. Proton Transport at the Interface of Subunit a in the Rotor Ring of E. Coli ATP Synthase, University of Wisconsin-Madison, 2010.

(9) Steed, P. R.; Fillingame, R. H. Subunit a Facilitates Aqueous Access to a Membrane-Embedded Region of Subunit c in Escherichia Coli F1F0 ATP Synthase. *J. Biol. Chem.* **2008**, *283* (18), 12365–12372. https://doi.org/10.1074/jbc.M800901200.

(10) Martin, J.; Hudson, J.; Hornung, T.; Frasch, W. D. F_o-Driven Rotation in the ATP Synthase Direction against the Force of F_1 ATPase in the $F_o F_1$ ATP Synthase. *J. Biol. Chem.* **2015**, *290* (17), 10717–10728. https://doi.org/10.1074/jbc.M115.646430.

(11) Lightowlers, R. N.; Howitt, S. M.; Hatch, L.; Gibson, F.; Cox, G. B. The Proton Pore in the Escherichia Coli F0F1-ATPase: A Requirement for Arginine at Position 210 of the a-Subunit. *BBA - Bioenerg.* **1987**, *894* (3), 399–406. https://doi.org/10.1016/0005-2728(87)90118-6.

(12) Jiang, W.; Fillingame, R. H. Interacting Helical Faces of Subunits a and c in the F1FO ATP Synthase of Escherichia Coli Defined by Disulfide Cross-Linking. *Proc. Natl. Acad. Sci. U. S. A.* **1998**, *95* (12), 6607–6612.

(13) Wiedenmann, A.; Dimroth, P.; von Ballmoos, C. $\Delta\psi$ and ΔpH Are Equivalent Driving Forces for Proton Transport through Isolated F0 Complexes of ATP Synthases. *Biochim. Biophys. Acta - Bioenerg.* **2008**, *1777* (10), 1301–1310. https://doi.org/10.1016/j.bbabio.2008.06.008.

(14) Preiss, L.; Langer, J. D.; Yildiz, O.; Eckhardt-Strelau, L.; Guillemont, J. E. G.; Koul, A.; Meier, T. Structure of the Mycobacterial ATP Synthase Fo Rotor Ring in Complex with the Anti-TB Drug Bedaquiline. *Sci. Adv.* **2015**, *1* (4), e1500106–e1500106. https://doi.org/10.1126/sciadv.1500106.

(15) Barik, S. Site-Directed Mutagenesis In Vitro by Megaprimer PCR. In *In Vitro Mutagenesis Protocols*; Humana Press: New Jersey, 1996; Vol. 57, pp 203–216. https://doi.org/10.1385/0-89603-332-5:203.

(16) Lowry, O. H.; Rosebrough, N. J.; Farr, A. L.; Randall, R. J. Protein Measurement with the Folin Phenol Reagent. *J. Biol. Chem.* **1951**, *193* (1), 265–275. https://doi.org/10.1016/0304-3894(92)87011-4.

(17) Moore, K. J.; Angevine, C. M.; Vincent, O. D.; Schwem, B. E.; Fillingame, R. H. The Cytoplasmic Loops of Subunit a of Escherichia Coli ATP Synthase May Participate in the Proton Translocating Mechanism. *J. Biol. Chem.* **2008**, *283* (19), 13044–13052. https://doi.org/10.1074/jbc.M800900200.